Inorganic Chemistry

Communication

pubs.acs.org/IC

New Facile Method for the Preparation of $M_3B_7O_{13}I$ Boracites (M = Mn, Fe, Co, Ni, Cd)

Xiu-Li Wang,[†,‡] Yi-Zhi Huang,[†] and Li-Ming Wu*[,†]

[†]State Key Laboratory of Structural Chemistry, Fujian Institute of Research on the Structure of Matter, Chinese Academy of Sciences, Fuzhou, Fujian 350002, People's Republic of China

[‡]University of Chinese Academy of Sciences, Beijing 100039, People's Republic of China

Supporting Information

ABSTRACT: Five iodine boracites, $M_3B_7O_{13}I$ (M = Mn, Fe, Co, Ni, Cd), have been synthesized by reactions of metal oxide, B_2O_3, element B, and I_2 at intermediate temperature above 350 °C. Powder X-ray diffraction analyses verify the identities and purity of the products, which are also confirmed by magnetic property measurement. Except safe, cheap, and convenient, this novel method is significantly flexible in the selection of the starting metal oxide. The influence of the reaction temperature and time has also been studied.

The unusual physical and chemical properties, such as ferroelectric, magnetic, dynamical, and structural properties[1] of boracites, $M_3B_7O_{13}X$ (M = divalent metals Mg, Cr, Mn, Fe, Co, Ni, Cu, Zn, Cd; X = usually Cl, Br, I), which represents a family of more than 25 isomorphous compounds, have been the focus of research for many years.[2] Usually, boracites have been prepared by four basic techniques, which include vapor-transport-type methods,[3,4] sintering-flux-type methods,[5,6] sol–gel processes,[7] and hydrothermal methods.[8] In the vapor-transport method, for example, HX and MX_2 acted as the gas-transport agent, as indicated by the represented reactions listed below:[3]

$$MO + 2HX(g) = MX_2(g) + H_2O(g)$$

$$6MX_2(g) + 7B_2O_3 + 5H_2O(g) = 2M_3B_7O_{13}X + 10HX(g)$$

whereas in a typical sintering-flux method boric acid acted as the flux:[6]

$$3CoCl_2\cdot 6H_2O + 7H_3BO_3 = Co_3B_7O_{13}Cl + 5HCl + 8H_2O$$

Hydrothermal methods were used for many systems that discovered chalcogen,[8] hydroxyl,[8,9] and lithium boracites,[9] but they were not suitable for halogen boracites.

The properties of iodine boracites are special among halogen boracites, such as direct coupling between the spontaneous electric polarization and magnetization in $Ni_3B_7O_{13}I$[10] and the tendency of the Curie temperature,[4,11] dielectric constant, and pyroelectric coefficient to increase on going from chlorine to iodine.[12] Yet, the aforementioned methods had several disadvantages: (i) the boracite products were contaminated with complex undesired byproducts, such as the partial incorporation of a hydroxyl group, which will lead to an undesirable increase of the switching field strength of boracites;[4] (ii) these methods need complex experimental techniques at elevated temperatures, typically reaching 900 °C, face a high risk of explosion or leakage of harmful gases, or require high pressure.[3,5,8] (iii) These techniques require transition-metal iodide as a starting reactant, such as MI_2 (M = Mn, Fe, Co, Ni, Cd), which are deliquescent or decompose in air. In addition, transition-metal iodides are generally expensive. Thus, a safe, facile, and inexpensive method for preparing halogen boracites is highly expected.

The newly established boron–sulfur method is a safe and convenient approach for the syntheses of a broad range of chalcogenides and oxychalcogenides[13−17] with easy experimental handling, mild experimental conditions under intermediate reaction temperature, below 500 °C, and normal pressure. The chalcogen sources are the in situ boron chalcogenides, which are loaded as boron and chalcogen elemental powders.[13−17] In this communication, we discovered that, starting with stoichiometric boron, iodine elements, and metal oxide, $M_3B_7O_{13}I$ (M = Mn, Fe, Co, Ni, Cd) are synthesized via the chemical combination reactions. We also show that this is a simple and clean approach to iodine boracites.

In brief, this new approach is a two-crucible method modified from the literature;[13−17] i.e., two silica crucibles were placed in a silica jacket: the top one contains stoichiometric metal oxide, B_2O_3, and the bottom one contains stoichiometric element boron and I_2. Then the reaction assembly was flame-sealed under vacuum, subsequently heated in a furnace to the designated reaction temperature in 2 h, held there for 3 days, and finally cooled to room temperature by switching off the furnace. To examine the effectiveness of this new procedure, five different boracites, $M_3B_7O_{13}I$ (M = Mn, Fe, Co, Ni, Cd), were synthesized. The experimental conditions and results are summarized in Table 1. Because of their similarity, only the experimental details on $Mn_3B_7O_{13}I$ (i.e., eq 1) are addressed: MnO (255 mg, 3.6 mmol), B_2O_3 (278 mg, 4.0 mmol), elemental boron (8 mg, 0.8 mmol), and I_2 (167 mg, 0.66 mmol) were weighed and loaded. Note that extra amounts of boron and I_2 according to the stoichiometry of eq 1 (Table 1) were loaded to ensure completeness of the reaction. The produced $Mn_3B_7O_{13}I$ was in

Received: September 17, 2012
Published: December 18, 2012

   dx.doi.org/10.1021/ic302018g | *Inorg. Chem.* 2013, 52, 9−11

Table 1. Reaction Conditions and Some Other Details of $M_3B_7O_{13}I$ (M = Mn, Fe, Co, Ni, Cd)

eq	loading ratio (mmol)[a]	reaction	product phase[b]/color/XRD	ref
1	3.6:4.0:0.8:0.66	$18MnO + 20B_2O_3 + 2B + 3I_2 \overset{450\ ^\circ C,\ 3\ days}{=} 6Mn_3B_7O_{13}I$	$Mn_3B_7O_{13}I$[d]/white/Figure 1a	18
2	1.8:3.4:3.2:0.66	$9Fe_2O_3 + 17B_2O_3 + 8B + 3I_2 \overset{400\ ^\circ C,\ 3\ days}{=} 6Fe_3B_7O_{13}I$	$Fe_3B_7O_{13}I$[d]/brown/Figure 1b	19
3	3.6:4.0:0.8:0.66	$18CoO + 20B_2O_3 + 2B + 3I_2 \overset{350\ ^\circ C,\ 3\ days}{=} 6Co_3B_7O_{13}I$	$Co_3B_7O_{13}I$[d]/cyan/Figure 1c	20
4	3.6:4.0:0.8:0.66	$18NiO + 20B_2O_3 + 2B + 3I_2 \overset{550\ ^\circ C,\ 3\ days}{=} 6Ni_3B_7O_{13}I$	$Ni_3B_7O_{13}I$[d]/brown/Figure 1d	21
5	3.6:4.0:0.8:0.66	$18CdO + 20B_2O_3 + 2B + 3I_2 \overset{400\ ^\circ C,\ 3\ days}{=} 6Cd_3B_7O_{13}I$	$Cd_3B_7O_{13}I$[d]/white/Figure 1e	c
6	1.2:3.6:2.4:0.66	$2Mn_3O_4 + 6B_2O_3 + 2B + I_2 \overset{450\ ^\circ C,\ 3\ days}{=} 2Mn_3B_7O_{13}I$	$Mn_3B_7O_{13}I$[d]/white/Figure S1 in the SI	18
7	1.2:3.6:2.4:0.66	$2Fe_3O_4 + 6B_2O_3 + 2B + I_2 \overset{400\ ^\circ C,\ 3\ days}{=} 2Fe_3B_7O_{13}I$	$Fe_3B_7O_{13}I$[d]/brown/Figure S2 in the SI	19
8	1.2:3.6:2.4:0.66	$2Co_3O_4 + 6B_2O_3 + 2B + I_2 \overset{350\ ^\circ C,\ 3\ days}{=} 2Co_3B_7O_{13}I$	$Co_3B_7O_{13}I$[d]/cyan/Figure S3 in the SI	20
9	3.6:4.0:0.8:0.66	$18MnO + 20B_2O_3 + 2B + 3I_2 \xrightarrow{400\ ^\circ C,\ 3\ days} Mn_3B_7O_{13}I + Mn_2B_6O_{11+x}$	mixture/brown/Figure S4a in the SI	18
10	3.6:4.0:0.8:0.66	$18MnO + 20B_2O_3 + 2B + 3I_2 \overset{500\ ^\circ C,\ 3\ days}{=} 6Mn_3B_7O_{13}I$	$Mn_3B_7O_{13}I$[d]/white/Figure S4b in the SI	18
11	3.6:4.0:0.8:0.66	$18MnO + 20B_2O_3 + 2B + 3I_2 \overset{600\ ^\circ C,\ 3\ days}{=} 6Mn_3B_7O_{13}I$	$Mn_3B_7O_{13}I$[d]/white/Figure S4c in the SI	18
12	3.6:4.0:0.8:0.66	$18MnO + 20B_2O_3 + 2B + 3I_2 \xrightarrow{600\ ^\circ C,\ 1\ day} Mn_2O_3 + Mn_3O_4 + I_2 + I_2O_4 + ?$	mixture/brown/Figure S5a in the SI	18
13	3.6:4.0:0.8:0.66	$18MnO + 20B_2O_3 + 2B + 3I_2 \overset{650\ ^\circ C,\ 1\ day}{=} 6Mn_3B_7O_{13}I$	$Mn_3B_7O_{13}I$[d]/white/Figure S5b in the SI	18
14	3.6:4.0:0.8:0.66	$18MnO + 20B_2O_3 + 2B + 3I_2 \overset{700\ ^\circ C,\ 1\ day}{=} 6Mn_3B_7O_{13}I$	$Mn_3B_7O_{13}I$[d]/white/Figure S5c in the SI	18
15	3.6:4.0:0.8:0.66	$18MnO + 20B_2O_3 + 2B + 3I_2 \overset{750\ ^\circ C,\ 1\ day}{=} 6Mn_3B_7O_{13}I$	$Mn_3B_7O_{13}I$[d]/white/Figure S5d in the SI	18
16	3.6:4.0:0:0.66	$18MnO + 20B_2O_3 + 3I_2 \xrightarrow{450\ ^\circ C,\ 3\ days} Mn(BO_2)_2 + I_2O_4$	mixture/brown/Figure S6a in the SI	
17	3.6:4.0:0:0.66	$18MnO + 20B_2O_3 + 3I_2 \xrightarrow{600\ C,\ 3\ days} Mn(BO_2)_2 + I_2O_4$	mixture/brown/Figure S6b in the SI	

[a]Loading ratio of $MnO:B_2O_3:B:I_2$ (mmol:mmol). [b]$Cd_3B_7O_{13}I$ crystallizes in $Pca2_1$; the remaining $M_3B_7O_{13}I$ (M = Mn, Fe, Co, Ni) crystallizes in cubic $F\bar{4}3c$. [c]$Cd_3B_7O_{13}I$: PDF-2 26-0247; unknown phase. [d]The yield based on metal oxides loaded is in the range of 70−95%; see the details in Table S1 in the SI.

a pure form (experimental details are listed in the Supporting Information, SI). X-ray diffraction (XRD) analyses indicated the purities of the products (after washing by distilled water and ethanol), and the XRD patterns were well indexed as cubic $F\bar{4}3c$ iodine boracites with parameters of 12.326(3), 12.2589(6), 12.093(4), and 11.998(5) Å for manganese (eq 1), iron (eq 2), cobalt (eq 3), and nickel (eq 4) iodine boracites, respectively, which are in good agreement with the literature values.[18−21] The only exception is $Cd_3B_7O_{13}I$ (eq 5), which crystallizes in orthorhombic $Pca2_1$ with a = 8.868(3) Å, b = 8.874(2) Å, and c = 12.507(4) Å and also agrees with that from PDF-2 data (PDF-2 26-0247). Figure 1 shows the representative XRD patterns, and others are shown in Figures S1−S5 in the SI. Note that $Mn_3B_7O_{13}I$ has been typically synthesized by a chemical-vapor-transport method at 800−900 °C;[11] our new approach only needs a considerably lower synthesis temperature that is nearly half of these values.

Considering the chemical reactions, three of the starting agents, MO, B_2O_3, and I_2, are obviously the sources of metal, boron, and iodine in the targeted $M_3B_7O_{13}I$ boracites; therefore, the necessity of the fourth starting agent, boron, may be in question. In order to probe this, two reactions (eqs 16 and 17), without loading boron compared to eqs 1 and 11, are designed (Table 1 and the SI) The XRD patterns indicated that, without boron, $M_3B_7O_{13}I$ could not be formed at all; only $Mn(BO_2)_2$ and I_2O_4 were observed (Figure S6 in the SI). These results ensure the important role of the boron element. We guess that it is the in situ formation of boron iodides[22] and their reactions in gaseous form with the metal oxide and B_2O_3 that generate $M_3B_7O_{13}I$. This proposed mechanism is deduced from that observed in the boron−sulfur method, during which the chalcogen sources are the in situ boron chalcogenides.[17,23] Further evidence is under investigation.

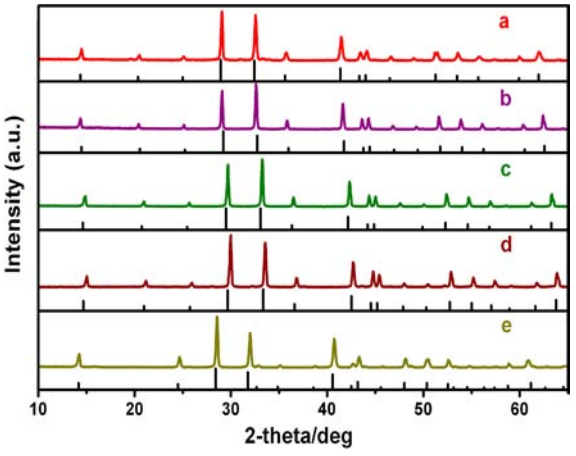

Figure 1. Powder XRD patterns of the as-synthesized boracites: (a) cubic $Mn_3B_7O_{13}I$ (eq 1); (b) cubic $Fe_3B_7O_{13}I$ (eq 2); (c) cubic $Co_3B_7O_{13}I$ (eq 3); (d) cubic $Ni_3B_7O_{13}I$ (eq 4); (e) orthorhombic $Cd_3B_7O_{13}I$ (eq 5).

dx.doi.org/10.1021/ic302018g | Inorg. Chem. 2013, 52, 9−11

A series of experiments (eqs 6−8 in Table 1) reveal that our new approach can also be a redox process, during which the starting 3+ transition-metal ion can be reduced by the in situ boron iodide into the 2+ ion in $M_3B_7O_{13}I$. For example, in reaction (6), starting Mn_3O_4 could be reduced at 450 °C to Mn^{2+} in the pure form of $Mn_3B_7O_{13}I$ under the same experimental conditions as those of MnO (eq 1 in Table 1). Similar phenomena were found for Fe_3O_4 (eq 7) versus Fe_2O_3 (eq 2) and Co_3O_4 (eq 8) versus CoO (eq 3). The experimental lattice parameters calculated by the cell refinement with the aid of JADE of the products from parallel reactions (for instance, those of eqs 1, 6, 10, 11, and 13−15) are consistent within experimental error (Table S1 in the SI). These indicate that the new approach is efficient regardless of the initial oxidation states of the metal atoms in the starting oxides. Such flexibility in the selection of starting oxides is reminiscent of the boron−sulfur method.[13]

In order to optimize the experimental conditions, the influence of the reaction temperature and time was examined. As listed in Table 1, eq 1 versus eqs 9−11 are the same reaction heated for 3 days at different temperatures, i.e., 450, 400, 500, and 600 °C, respectively. As indicated by the XRD patterns, upon heating at 400 °C, reaction (9) had not been completed yet, because other than the targeted $Mn_3B_7O_{13}I$, an impurity, $Mn_2B_6O_{11+x}$, has also been detected (Figure S4a in the SI). Reactions (10) and (11) at elevated temperature, 500 and 600 °C, both produce pure phase $Mn_3B_7O_{13}I$ with different degrees of crystallinity. At a higher temperature of 600 °C, the half-width of the diffraction peak decreases (part b versus c in Figure S4b in the SI) and the morphology of the product is improved (Figure S7 in the SI) The scanning electron microscopy images shown in Figure S7 in the SI also indicate that the products are in a regular cubiclike shape with an edge size of about several micrometers to 10 μm. With an increase of the reaction temperature, the number of irregular smaller particles on the surface decreases, and the monodispersity of the product in size and shape is improved.

Another batch of reactions were designed to probe the influence of the reaction time. As listed in Table 1, reaction (9) indicates that, at 400 °C for 3 days, the reaction has not been completely converted to $Mn_3B_7O_{13}I$ yet; a second phase $Mn_2B_6O_{11+x}$ was also found. Whereas reaction (12) suggests that, at 600 °C for 1 day, $Mn_3B_7O_{13}I$ is not formed at all, only a mixture of simple binaries, Mn_2O_3, Mn_3O_4, and I_2O_4, together with one of the loading reactants, I_2, was found (Figure S5a in the SI). Evidently, heating for only 1 day is not enough. Equations 13−15 reveal that, within 1 day, $Mn_3B_7O_{13}I$ occurs as a pure phase only at/or above 650 °C (Figure S5b−d in the SI). Finally, the optimized experimental conditions for $Mn_3B_7O_{13}I$ are established as starting from the reactants of MnO, B_2O_3, boron, and I_2 with a loading ratio of 36:40:8:6.6 and heating at 450 °C for 3 days (eq 1 and the SI).

To verify the purity of the as-synthesized $Mn_3B_7O_{13}I$ and the oxidation state of its manganese cation, the magnetic susceptibility has been measured. The product of eq 1 has been selected as a representative. Figure S8 in the SI shows a typical magnetic behavior for the Mn^{2+} ion, following the Curie−Weiss law at high temperatures, and an antiferromagnetic interaction between Mn^{2+} ions at low temperature. The calculated effective magnetic moment is 10.93 μ_B, which agrees reasonably well with the theoretical value of 10.25 μ_B of spin-only Mn^{2+} ions.[24]

In conclusion, we have reported a new facile method for the preparation of $M_3B_7O_{13}I$. This method is novel and shows several advantages: (1) safer and convenient handling; all of the starting reactants are stable chemically in air; (2) cheap considering the prices of metal oxide versus metal iodide required by other methods; (3) low risk of leakage of harmful gas; (4) flexible in choosing metal oxide with different oxidation states as the starting agent; (5) mild reaction conditions; this method needs considerably lower reaction temperature, e.g., 450 versus 900 °C for $Mn_3B_7O_{13}I$ with respect to the chemical-vapor-transport method; (6) promising for a wider application on the syntheses of other boracites formed by transition metals other than Mn, Fe, Co, Ni, and Cd reported here, main-group metals, and lighter halogens (Cl and Br) or chalcogens (S, Se, and Te).

■ ASSOCIATED CONTENT

Supporting Information

Additional tables and figures. This material is available free of charge via the Internet at http://pubs.acs.org.

■ AUTHOR INFORMATION

Corresponding Author

*E-mail: liming_wu@fjirsm.ac.cn. Tel: (011)86-591-83705401.

Notes

The authors declare no competing financial interest.

■ ACKNOWLEDGMENTS

This research was supported by the 973 Program (Grant 2010CB933501) and National Natural Science Foundation of China under Projects 20973175, 21103190, and 21233009.

■ REFERENCES

(1) Nelmes, R. J. *J. Phys. C: Solid State Phys.* **1974**, *7*, 3840.
(2) Campa-Molina, J.; Blanco, O.; Correz-Gomez, A.; Czank, M.; Castellanos-Guzman, A. G. *J. Microsc. (Oxford, U.K.)* **2002**, *208*, 201.
(3) Schmid, H. *J. Phys. Chem. Solids* **1965**, *26*, 973.
(4) Schmid, H.; Tippman, H. *J. Cryst. Growth* **1979**, *46*, 723.
(5) Jona, F. *J. Phys. Chem.* **1959**, *63*, 1750.
(6) Zagudailova, M. B.; Plachinda, P. A.; Berdonosov, P. S.; Stefanovich, S. Y.; Dolgikh, V. A. *Inorg. Mater.* **2005**, *41*, 393.
(7) Nagase, T.; Sakane, K.; Wada, H. *J. Sol−Gel Sci. Technol.* **1998**, *13*, 223.
(8) Joubert, J.; Muller, J.; Fouassier, C.; Levasseur, A. *Krist. Tech.* **1971**, *6*, 65.
(9) Werthmann, U.; Gies, H.; Glinnemann, J.; Hahn, Th. *Z. Kristallogr.* **2000**, *215*, 393.
(10) Schmid, H. *Ferroelectrics* **1999**, *221*, 9.
(11) Crottaz, O.; Schobinger-Papamantellos, P.; Suard, E.; Ritter, C.; Gentil, S.; Rivera, J. P.; Schmid, H. *Ferroelectrics* **1997**, *204*, 45.
(12) Castellanosguzman, A. G.; Burfoot, J. C.; Schmid, H.; Tissot, P. *Ferroelectrics* **1981**, *36*, 411.
(13) Wu, L. M.; Seo, D. K. *J. Am. Chem. Soc.* **2004**, *126*, 4676.
(14) Huang, Y. Z.; Wu, L. M.; Du, S. W.; Chen, L. *Inorg. Chem.* **2009**, *48*, 3901.
(15) Huang, Y. Z.; Chen, L.; Wu, L. M. *Inorg. Chem.* **2008**, *47*, 10723.
(16) Huang, Y. Z.; Chen, L.; Wu, L. M. *Cryst. Growth Des.* **2008**, *8*, 739.
(17) Wu, L. M.; Sharma, R.; Seo, D. K. *Inorg. Chem.* **2003**, *42*, 5798.
(18) Crottaz, O.; Kubel, F.; Schmid, H. J. *Solid State Chem.* **1995**, *120*, 60.
(19) Kubel, F. *Ferroelectrics* **1994**, *160*, 61.
(20) Becker, W. J.; Will, G. *Z. Kristallogr.* **1970**, *131*, 139.
(21) Saifuddinov, V. Z.; Bugakov, V. I.; Pakhomov, V. I. *Inorg. Mater.* **1980**, *16*, 112.
(22) Ring, M. A.; Donnay, J. D. H.; Koski, W. S. *Inorg. Chem.* **1962**, *1*, 109.
(23) Chen, H.-Y.; Gilles, P. W. *J. Am. Chem. Soc.* **1970**, *92*, 2309.
(24) Oconnor, C. J. *Prog. Inorg. Chem.* **1982**, *29*, 203.